

# POINT CONFIGURATIONS AND COXETER OPERADS

SUZANNE M. ARMSTRONG, MICHAEL CARR, SATYAN L. DEVADOSS, ERIC ENGLER, ANANDA LEININGER, AND MICHAEL MANAPAT

ABSTRACT. The minimal blow-ups of simplicial Coxeter complexes are natural generalizations of the real moduli space of Riemann spheres. They inherit a tiling by the graph-associahedra convex polytopes. We obtain explicit configuration space models for the classical infinite families of finite and affine Weyl groups using particles on lines and circles. A Fulton-MacPherson compactification of these spaces is described and this is used to define a *Coxeter operad*. A complete classification of the building sets of these complexes is also given with a computation of their Euler characteristics.

## 1. MOTIVATION FROM PHYSICS

1.1. A configuration space of  $n$  ordered, distinct particles on a variety  $V$  is

$$C_n(V) = V^n - \Delta, \quad \text{where } \Delta = \{(x_1, \dots, x_n) \in V^n \mid \exists i, j, x_i = x_j\}.$$

Over the past decade, there has been an increased interest in the configuration space of  $n$  labeled points on the projective line. The focus is on a quotient of this space by  $\mathbb{P}\mathrm{GL}_2(\mathbb{C})$ , the affine automorphisms on  $\mathbb{CP}^1$ . The resulting variety is the moduli space of Riemann spheres with  $n$  punctures

$$\mathcal{M}_{0,n} = C_n(\mathbb{CP}^1)/\mathbb{P}\mathrm{GL}_2(\mathbb{C}).$$

There is a compactification  $\overline{\mathcal{M}}_{0,n}$  of this space, a smooth variety of complex dimension  $n - 3$ , coming from Geometric Invariant Theory [22].

This Deligne-Knudsen-Mumford compactification allows collisions of points, whose description comes from the repulsive potential observed by quantum physics: Pushing particles together creates a spherical bubble onto which the particles escape [23]. In other words, as points try to collide, the result is a new bubble fused to the old at the point of collision, where the collided points are now on the new bubble. The phenomena is dubbed as *bubbling*, with the resulting structure as a bubble-tree. The space  $\overline{\mathcal{M}}_{0,n}$  plays a crucial role as a fundamental building block in the theory of Gromov-Witten invariants, also appearing in symplectic geometry and quantum cohomology [19].

Our work is motivated by the *real* points  $\overline{\mathcal{M}}_{0,n}(\mathbb{R})$  of this space, the set of points fixed under complex conjugation. These real moduli spaces have importance in their own right, and are beginning to appear in other areas such as  $\zeta$ -motives [16], phylogenetic trees [1], and Lagrangian Floer theory [14].

It was Kapranov [18] who first noticed a relationship between  $\overline{\mathcal{M}}_{0,n}(\mathbb{R})$  and the braid arrangement of hyperplanes, associated to the Coxeter group of type  $A_n$ : Blow-ups of certain cells of the

---

1991 *Mathematics Subject Classification*. Primary 52C35, Secondary 14P25, 52B11.

All authors were partially supported by NSF grant DMS-9820570. Carr and Devadoss were also supported by NSF CARGO grant DMS-0310354.

$A_n$  Coxeter complex yields a space homeomorphic to a double cover of  $\overline{\mathcal{M}}_{0,n+2}(\mathbb{R})$ . This creates a natural tiling of  $\overline{\mathcal{M}}_{0,n}(\mathbb{R})$  by associahedra, the combinatorics of which is discussed in [12]. Davis et. al have generalized this to all Coxeter groups [7], along with studying the fundamental groups of these blown-up spaces [8]. Carr and Devadoss [5] looked at the simplicial Coxeter groups with the inherent tiling of these spaces by the convex polytopes *graph-associahedra*.

1.2. Our goal is to give an explicit configuration space analog of these blown-up Coxeter complexes. Our attention will be restricted to the classical infinite families of simplicial Coxeter groups, which generalize to arbitrary number of generators (of type  $A, B, D, \tilde{A}, \tilde{B}, \tilde{C}, \tilde{D}$ ). This is done in order to mimic the structure of  $\mathcal{M}_{0,n}(\mathbb{R})$ , as well as to provide an operad structure.

Section 2 provides the background of Coxeter groups and their associated Coxeter complexes. In Section 3, we construct our configuration spaces associated to the complexes. Section 4 introduces the bracketing notation in order to visualize collisions in the configuration spaces, leading to viewing the hyperplanes of the Coxeter complexes in this new language. It is this notation that provides a transparent understanding and straight-forward proofs to several results in this paper. In particular, it allows for a complete classification of the minimal building sets for the Coxeter complexes, along with their enumeration, as given in Tables 3 and 4.

The Fulton-MacPherson compactification [15] of these spaces is discussed in Section 5. This is used to define the notion of a *Coxeter operad*. Here, *nested* bracketing are used to describe the structure of the compactified spaces, enabling us to describe how the chambers of these spaces glue together. Section 6 ends with combinatorial results using the theory developed in [5]. For instance, the Euler characteristic of the blown-up Coxeter complexes is given, exploiting the tilings by graph-associahedra.

*Acknowledgments.* We express our gratitude to Martin Markl and Jim Stasheff for sharing their knowledge about the operad literature, as well as offering guidance and encouragement. Our thanks also go to Tom Garrity and Vic Reiner for helpful discussions. Finally, it is our pleasure to thank Alex Postnikov for working on the  $f$ -vectors of graph-associahedra on our behalf.

## 2. SPHERICAL AND EUCLIDEAN COMPLEXES

2.1. This section will present background, namely standard facts and definitions about Coxeter systems. Most of the material here can be found in Bourbaki [3] and Brown [4].

**Definition 2.1.** Given a finite set  $S$ , a *Coxeter group*  $W$  is given by the presentation

$$W = \langle s_i \in S \mid s_i^2 = 1, (s_i s_j)^{m_{ij}} = 1 \rangle,$$

where  $m_{ij} = m_{ji}$  and  $2 \leq m_{ij} \leq \infty$ . The pair  $(W, S)$  is called a *Coxeter system*.

Associated to any Coxeter system  $(W, S)$  is its *Coxeter graph*  $\Gamma_W$ : Each node represents an element of  $S$ , where two nodes  $s_i, s_j$  determine an edge if and only if  $m_{ij} \geq 3$ . A Coxeter group is *irreducible* if its Coxeter graph is connected and it is *locally finite* if either  $W$  is finite or each proper subset of  $S$  generates a finite group. A Coxeter group is *simplicial* if it is irreducible and locally finite

[8, Section 7.3]. The classification of simplicial Coxeter groups and their Coxeter graphs are well-known [3, Chapter 6].

We restrict our attention to infinite families of simplicial Coxeter groups which generalize to arbitrary number of generators. This will mimic configuration spaces of an arbitrary number of particles since our motivation comes from  $\overline{\mathcal{M}}_{0,n}(\mathbb{R})$ . There are only seven such types of Coxeter groups: three spherical ones and four Euclidean ones. Figure 1 shows the Coxeter graphs associated to the Coxeter groups of interest; we label the edge with its order for  $m_{ij} > 3$ . The number of nodes of a graph is given by the subscript  $n$  for the spherical groups, whereas the number of nodes is  $n + 1$  for the Euclidean case.

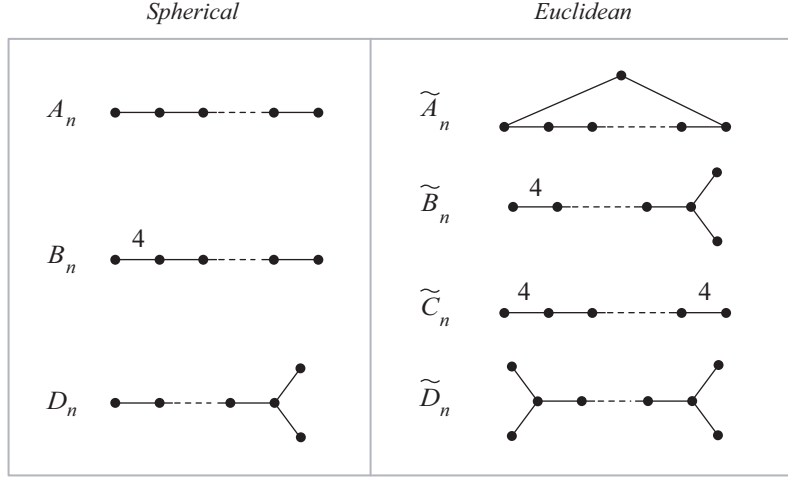


FIGURE 1. Coxeter graphs of simplicial spherical and Euclidean groups.

2.2. Every spherical Coxeter group has an associated finite reflection group realized by reflections across linear hyperplanes on a sphere. Every conjugate of a generator  $s_i$  acts on the sphere as a reflection in some hyperplane, dividing the sphere into simplicial chambers. The sphere, along with its cellulation is the *Coxeter complex* corresponding to  $W$ , denoted  $CW$ . The hyperplanes associated to each group given in Table 1 lie on the  $(n - 1)$  sphere. The  $W$ -action on the chambers of  $CW$  is simply transitive, and thus we may associate an element of  $W$  to each chamber; generally, the identity is associated to the fundamental chamber. Thus the number of chambers of  $CW$  comes from the order of the group.

| $W$   | Hyperplanes              | # Chambers   |
|-------|--------------------------|--------------|
| $A_n$ | $x_i = x_j$              | $(n + 1)!$   |
| $B_n$ | $x_i = \pm x_j, x_i = 0$ | $2^n n!$     |
| $D_n$ | $x_i = \pm x_j$          | $2^{n-1} n!$ |

TABLE 1. The spherical complexes.

Figure 2(a) is  $\mathcal{CA}_3$ , the 2-sphere with hyperplane markings, and Figure 2(b) is the 2-sphere  $\mathcal{CB}_3$ . Note that both of them are tiled by 2-simplices.



FIGURE 2. Coxeter complexes (a)  $\mathcal{CA}_3$  and (b)  $\mathcal{CB}_3$ .

2.3. We move from spherical geometry coming from linear hyperplanes to Euclidean geometry arising from affine hyperplanes. Just as with the spherical case, each Euclidean Coxeter group has an associated Euclidean reflection group realized as reflections across affine hyperplanes in Euclidean space. Again, we focus on the infinite families of such Euclidean Coxeter groups which are  $\tilde{A}_n$ ,  $\tilde{B}_n$ ,  $\tilde{C}_n$ , and  $\tilde{D}_n$ . The hyperplanes<sup>1</sup> associated to each group, given in Table 2, lie in  $\mathbb{R}^n$ .

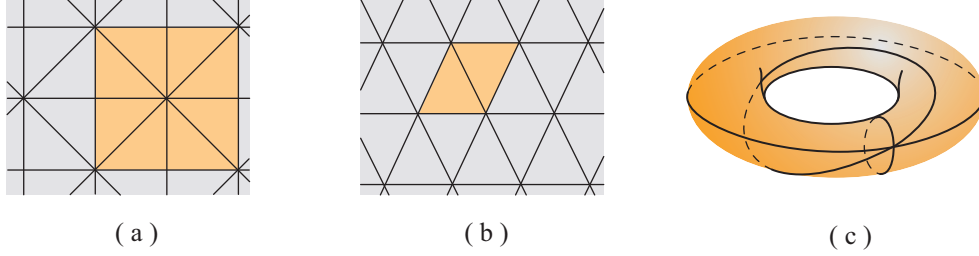
| $W$           | Hyperplanes ( $k \in 2\mathbb{Z}$ )           | # Chambers   |
|---------------|---|--------------|
| $\tilde{A}_n$ | $x_i = x_j + k$                               | $n!$         |
| $\tilde{B}_n$ | $x_i = \pm x_j + k, x_i = 1 + k$              | $2^{n-1} n!$ |
| $\tilde{C}_n$ | $x_i = \pm x_j + k, x_i = 1 + k, x_i = 0 + k$ | $2^n n!$     |
| $\tilde{D}_n$ | $x_i = \pm x_j + k$                           | $2^{n-2} n!$ |

TABLE 2. The toroidal complexes.

We look at the quotient of the Euclidean space  $\mathbb{R}^n$  by a group of translations, resulting in the  $n$ -torus  $\mathbb{T}^n$ . This is done for three reasons: First, the configuration space model is a more natural object after the quotient, resulting in particles on circles. Second, it is the correct generalization of the affine type  $A$  complex, as discussed in [11]. Third, and most importantly, it presents us with a valid operad structure.

The translations for  $\tilde{A}_n$  are covered in [11, Section 2.3]. For the remaining cases, we choose coordinate translations of magnitude 2. This has the benefit of identifying the most ubiquitous set of hyperplanes  $\{x_i = \pm x_j + k\}$ , producing an arrangement that is familiar from the spherical cases. We refer to the quotient of the Coxeter complex  $\mathcal{CW}$  of Euclidean type as the *toroidal Coxeter complex*, denoted as  $\mathbb{TCW}$ . Figure 3(a) shows the hyperplanes of  $\tilde{C}_2$  in  $\mathbb{R}^2$ , whereas (b) shows the hyperplanes for  $\tilde{A}_2$ . Figure 3(c) is the cellulation of the toroidal complex  $\mathbb{TC}\tilde{A}_2$ .

<sup>1</sup>We choose a slightly non-standard collection of hyperplanes in order for the associated configuration spaces to be more canonical.

FIGURE 3. Coxeter complexes (a)  $\mathcal{C}\tilde{C}_2$ , (b)  $\mathcal{C}\tilde{A}_2$  and (c)  $\mathbb{TC}\tilde{A}_2$ .

### 3. CONFIGURATION SPACES

3.1. We now give an explicit configuration space analog to each Coxeter complex above. These appear as (quotients of) configuration spaces of particles on the line  $\mathbb{R}$  and the circle  $\mathbb{S}$ . The arguments used for the constructions below are elementary, immediately following from the hyperplane arrangements of the reflection groups. However, as shown in Section 5, the configuration space model we provide will enable us to elegantly capture the blow-ups of these Coxeter complexes.

**Definition 3.1.** Let  $C_n(\mathbb{R}) = \mathbb{R}^n - \{(x_1, x_2, \dots, x_n) \in \mathbb{R}^n \mid \exists i, j, x_i = x_j\}$  be the configuration space of  $n$  labeled particles on the real line  $\mathbb{R}$ . A generic point in  $C_5(\mathbb{R})$  is  $x_1 < x_2 < x_3 < x_4 < x_5$ , which we notate (without labels) as  $\bullet - \bullet - \bullet - \bullet - \bullet$ .

**Definition 3.2.** Let  $C_{\bar{n}}(\mathbb{R}_{\bullet}) = \mathbb{R}^n - \{(x_1, x_2, \dots, x_n) \in \mathbb{R}^n \mid \exists i, j, x_i = \pm x_j \text{ or } x_i = 0\}$  be the space of  $n$  pairs of *symmetric* labeled particles (denoted  $\bar{n}$ ) across the origin. A point in  $C_3(\mathbb{R}_{\bullet})$  is  $-x_3 < -x_2 < -x_1 < 0 < x_1 < x_2 < x_3$ , which is depicted without labels as  $\circ - \circ - \circ - \bullet - \circ - \circ - \circ$ , where the black particle is fixed at the origin.

**Definition 3.3.** Let  $C_{\bar{n}}(\mathbb{R}_o) = \mathbb{R}^n - \{(x_1, x_2, \dots, x_n) \in \mathbb{R}^n \mid \exists i, j, x_i = \pm x_j\}$  be the space of  $\bar{n}$  pairs of symmetric labeled particles across the origin, where the particle  $x_i$  and its symmetric pair  $-x_i$  are both allowed to occupy the origin. A point in  $C_3(\mathbb{R}_o)$  is

$$(3.1) \quad -x_3 < -x_2 < -x_1, x_1 < x_2 < x_3$$

drawn  $\circ - \circ - \circ - + - \circ - \circ$  without labels. Notice the mark at the origin where there is no fixed particle: The point  $-x_3 < -x_2 < x_1, -x_1 < x_2 < x_3$  drawn as  $\circ - \circ - \circ - + - \circ - \circ$  lies in the same chamber of  $C_3(\mathbb{R}_o)$  as Eq.(3.1).

Let  $\text{Aff}(\mathbb{R})$  be the group of affine transformations of  $\mathbb{R}$  generated by translating and positive scaling. The action of  $\text{Aff}(\mathbb{R})$  on  $C_n(\mathbb{R})$  translates the leftmost of the  $n$  particles in  $\mathbb{R}$  to  $-1$  and the rightmost is scaled to 1. Taking the closure of this configuration space allows particles to *collide* (coincide with each other) on the line.

**Proposition 3.4.** Let  $C_n\langle\mathbb{R}\rangle$  denote the closure of  $C_n(\mathbb{R})/\text{Aff}(\mathbb{R})$ . Then  $C_n\langle\mathbb{R}\rangle$  has the same cellulation as  $CA_{n-1}$ .

A detailed proof of this is given in [12, Section 4]. Roughly, quotienting by translations of  $\text{Aff}(\mathbb{R})$  removes the inessential component of the arrangement and scaling results in restricting to the sphere  $\mathcal{CA}_{n-1}$ .

The proposition above can be extended to the other spherical Coxeter complexes. Let  $\text{Aff}(\bar{\mathbb{R}})$  be the transformations of  $\mathbb{R}$  generated simply by positive scalings: The action of  $\text{Aff}(\bar{\mathbb{R}})$  scales the (symmetric) particles farthest from the origin to unit distance. Let  $C_{\bar{n}}\langle\mathbb{R}_{\bullet}\rangle$  and  $C_{\bar{n}}\langle\mathbb{R}_{\circ}\rangle$  denote the closures of  $C_{\bar{n}}(\mathbb{R}_{\bullet})/\text{Aff}(\bar{\mathbb{R}})$  and  $C_{\bar{n}}(\mathbb{R}_{\circ})/\text{Aff}(\bar{\mathbb{R}})$  respectively.

**Proposition 3.5.**  *$C_{\bar{n}}\langle\mathbb{R}_{\bullet}\rangle$  and  $C_{\bar{n}}\langle\mathbb{R}_{\circ}\rangle$  have the same cellulation as  $\mathcal{CB}_n$  and  $\mathcal{CD}_n$  respectively.*

*Proof.* From the above definition above, it is clear  $C_{\bar{n}}(\mathbb{R}_{\bullet})$  and  $C_{\bar{n}}(\mathbb{R}_{\circ})$  are complements of the hyperplanes given in Table 1. The closure of the spaces simply include the hyperplanes back into  $\mathbb{R}^n$ . Thus any collision in the closed configuration space maps to a point on the hyperplanes defined by the associated finite reflection group. Quotienting by  $\text{Aff}(\bar{\mathbb{R}})$  allows choosing a particular representative for each fiber. Specifically, for the fiber containing  $(x_1, x_2, \dots, x_n)$ , choose

$$(x_1, x_2, \dots, x_n) / \sqrt{x_1^2 + x_2^2 + \dots + x_n^2},$$

giving a map onto the unit sphere in  $\mathbb{R}^n$ . The cellulation of the sphere by these hyperplanes yields the desired Coxeter complex.  $\square$

3.2. We move from the spherical to the affine (toroidal) complexes. However, the interest now is on configurations of particles on the circle  $\mathbb{S}$ . The group of rotations acts freely on  $C_n(\mathbb{S})$ , and its quotient is denoted by  $C_n(\mathbb{S}')$ ; Figure 4(a) shows a point in  $C_9(\mathbb{S}')$  drawn without labels.

**Proposition 3.6.** *The closure  $C_{\bar{n}}\langle\mathbb{S}'\rangle$  of  $C_n(\mathbb{S}')$  has the same cellulation as  $\text{TC}\tilde{A}_{n-1}$ .*

A proof of this is given in [11, Section 3]. A similar construction is produced below for the other three toroidal Coxeter complexes. Our focus is on the circle  $\mathbb{S}$  with the vertical line through its center as its axis of symmetry, where the two diametrically opposite points on the axis are labeled 0 and 1. The space of interest is the configuration space of pairs of *symmetric* labeled particles (again denoted  $\bar{n}$ ) across this symmetric axis of the circle.

**Definition 3.7.** Let  $C_{\bar{n}}(\mathbb{S}_{\circ}^{\bullet}) = \mathbb{T}^n - \{(x_1, x_2, \dots, x_n) \in \mathbb{T}^n \mid \exists i, j, x_i = \pm x_j \text{ or } x_i = 1\}$  be the space of  $n$  pairs of symmetric labeled particles on  $\mathbb{S}$  with a fixed particle at 1. Figure 4(b) shows a point in  $C_5(\mathbb{S}_{\circ}^{\bullet})$ .

**Definition 3.8.** Let  $C_{\bar{n}}(\mathbb{S}_{\bullet}^{\circ}) = \mathbb{T}^n - \{(x_1, x_2, \dots, x_n) \in \mathbb{T}^n \mid \exists i, j, x_i = \pm x_j \text{ or } x_i = 1 \text{ or } x_i = 0\}$  be the space of  $n$  pairs of symmetric labeled particles on  $\mathbb{S}$  with a fixed particle at 0 and 1. Figure 4(c) shows a point in  $C_5(\mathbb{S}_{\bullet}^{\circ})$ .

**Definition 3.9.** Let  $C_{\bar{n}}(\mathbb{S}_{\circ}^{\circ}) = \mathbb{T}^n - \{(x_1, x_2, \dots, x_n) \in \mathbb{T}^n \mid \exists i, j, x_i = \pm x_j\}$  be the space of  $n$  pairs of symmetric labeled particles on  $\mathbb{S}$  with no fixed particles. Figure 4(d) shows a point in  $C_5(\mathbb{S}_{\circ}^{\circ})$ .

**Proposition 3.10.** *The closures  $C_{\bar{n}}\langle\mathbb{S}_{\circ}^{\bullet}\rangle$ ,  $C_{\bar{n}}\langle\mathbb{S}_{\bullet}^{\circ}\rangle$  and  $C_{\bar{n}}\langle\mathbb{S}_{\circ}^{\circ}\rangle$  have the same cellulation as  $\text{TC}\tilde{B}_n$ ,  $\text{TC}\tilde{C}_n$  and  $\text{TC}\tilde{D}_n$  respectively.*

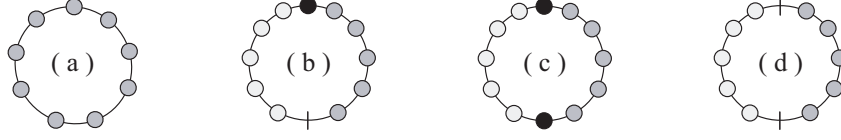


FIGURE 4. Configurations of particles (a) without and (b) - (d) with symmetry.

*Proof.* This is a direct consequence of the definitions of the configuration spaces, of the toroidal complexes, and their corresponding hyperplane arrangements given in Table 2.  $\square$

3.3. The group of reflections  $W$  across the respective hyperplanes acts on the configuration space by permuting particles. Let  $\sigma(W)$  denote the group acting *simply transitively* on the configuration spaces above. As mentioned above, for the spherical complexes,  $\sigma(W)$  is isomorphic to  $W$ . The (symmetric) group  $\sigma(A_n)$  is generated by transpositions  $s_{ij}$  which interchange the  $i$ -th and  $j$ -th particle. The Coxeter group  $B_n$  of *signed permutations* is generated by  $s_{ij}$  along with reflections  $r_1, \dots, r_n$ , where  $r_i$  changes the sign of the  $i$ -th particle. Note that  $B_n$  is isomorphic to  $\mathbb{Z}_2^n \rtimes \mathbb{S}_n$ .

The Coxeter group  $D_n$  is classically represented as the group of *even* signed permutations. Alternatively,  $D_n$  is isomorphic to the group  $\mathbb{Z}_2^{n-1} \rtimes \mathbb{S}_n$ , generated by transpositions  $s_{ij}$  along with reflections  $r_2, \dots, r_n$ . From the configuration space model  $C_n(\mathbb{R}_o)$ , the missing reflection  $r_1$  corresponds to the reflection of the particle and its inverse closest to the origin.

Although the spherical groups  $W$  act simply transitively on their configuration spaces, the action of the affine groups is only transitive on the toroidal complexes. The simplest way to compute  $\sigma(W)$  for the toroidal cases is from observing the diagrams given in Figure 4. Cutting the circle along a fixed point and “laying it flat” gives us the appropriate groups. Since a point of  $C_n(\mathbb{S}')$  is fixed by the group of rotations, then  $\sigma(\tilde{A}_n)$  is isomorphic to  $A_{n-1}$ . Similarly,  $\sigma(\tilde{B}_n)$  is isomorphic to  $D_n$  and  $\sigma(\tilde{C}_n)$  is isomorphic to  $B_n$ . The group  $\sigma(\tilde{D}_n)$  is generated by transpositions  $s_{ij}$  along with reflections  $r_2, \dots, r_{n-1}$ . Similar to the  $D_n$  case above, the missing elements  $r_1$  and  $r_n$  correspond to the reflections along the centrally symmetric axis. The group  $\sigma(\tilde{D}_n)$  is isomorphic to  $\mathbb{Z}_2^{n-2} \rtimes \mathbb{S}_n$ .

#### 4. BRACKETINGS AND HYPERPLANES

4.1. We introduce the bracket notation in order to visualize collisions in the closed configuration spaces. This notation will lead to a transparent understanding and to straight-forward proofs of our results below. In particular, Proposition 4.7 produces a complete classification of the minimal building sets for the Coxeter complexes, along with their enumeration, as given in Tables 3 and 4.

A *bracket* is drawn around adjacent particles on a configuration space diagram representing the collision of the included particles. A *k-bracketing* of a diagram is a set of  $k$  brackets representing multiple independent particle collisions. For example, the configuration

$$(4.1) \quad -x_4 = -x_3 < -x_2 < -x_1 = 0 = x_1 < x_2 < x_3 = x_4$$

in  $C_5(\mathbb{R}_\bullet)$  corresponds to the bracketing Each bracket on a configuration space diagram with symmetric particles will actually consist of two symmetric brackets, one on

each side of the origin, with this symmetric pair counting as only one bracket. If this set includes the origin, we draw one symmetric bracket around the origin, which again counts as one bracket. Thus Eq.(4.1) is a 2-bracketing of its diagram.

We define the *support* of a bracketing to be the configuration space associated to the bracketing diagram; it is the subspace (of the configuration space) in which particles that share a bracket have collided. However, a set of collisions in a configuration space defines an intersection of hyperplanes. So, alternatively, the support of a bracketing is the smallest intersection of hyperplanes associated to the bracketing.

**Example 4.1.** Figure 5 shows part of the two-dimensional complexes  $\mathcal{CB}_3$  and  $\mathcal{CD}_3$ , one with a fixed particle at the axis of symmetry  $C_3\langle\mathbb{R}_\bullet\rangle$  and one without  $C_3\langle\mathbb{R}_\circ\rangle$ . As we move through the chambers, going from (a) through (g), a representative of each configuration is shown. Notice that since there is no fixed particle at the axis of symmetry for type  $D$ , there is no meaningful bracketing of the symmetric particles closest to the axis; they may pass each other freely *without* collision.

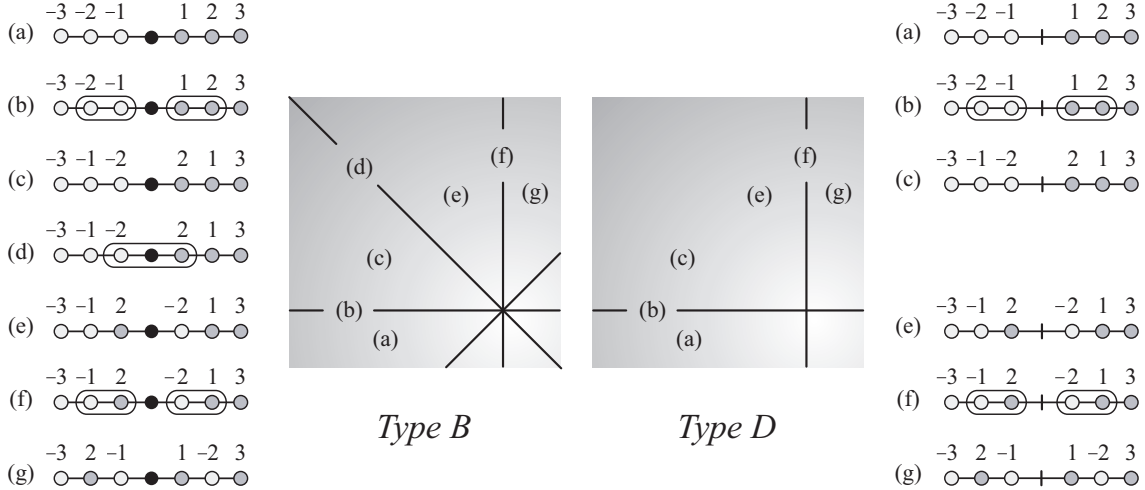


FIGURE 5. Local regions of  $\mathcal{CB}_3$  and  $\mathcal{CD}_3$ .

4.2. Given a set of hyperplanes of either a sphere or affine space  $V$ , let  $\alpha$  be an intersection of hyperplanes in  $V$ . We say that hyperplanes  $h_i$  *cellulate*  $\alpha$  to mean the intersections  $h_i \cap \alpha$  cellulate  $\alpha$ . Denote by  $\mathcal{H}_s \alpha$  the set of all hyperplanes that contain  $\alpha$ . If reflections in these hyperplanes generate a finite reflection group, it is called the *stabilizer* of  $\alpha$ . Note that in a simplicial Coxeter complex, the stabilizer exists for all intersections of hyperplanes.<sup>2</sup>

Let  $G$  be a  $k$ -bracketing diagram and let  $\alpha$  be the support of  $G$ . One can determine the stabilizing hyperplanes of  $\alpha$  using the following lemma, which comes straight from the definition.

<sup>2</sup>By abuse of terminology, we also refer to the set  $\mathcal{H}_s \alpha$  as the stabilizer of  $\alpha$ .




**Lemma 4.2.** *If  $\alpha$  is the support of a bracketing  $G$ , then for every pair of particles  $x_i$  and  $x_j$  that share a bracket in  $G$ , the hyperplane defined by  $x_i = x_j$  is in  $\mathcal{H}_s\alpha$ .*

The hyperplanes of the cellulation of  $\alpha$  represent all possible collisions of pairs of particles in that configuration space. When redundancies are accounted for, the cellulation of  $\alpha$  emerges with a natural configuration space structure.

**Lemma 4.3.** *If  $\alpha$  is the support of a bracketing  $G$ , then the cellulation of  $\alpha$  is the configuration space of a diagram  $H$ , which is obtained from  $G$  by replacing each bracket with a particle.*

*Proof.* The cellulation of  $\alpha$  is determined by the hyperplanes of  $\alpha$ , which are simply the intersections of hyperplanes of  $W$  with  $\alpha$ . If the particles  $x_i$  and  $x_j$  share a bracket in  $\alpha$ , then  $x_k$  cannot collide with  $x_j$  in  $\alpha$  without also colliding with  $x_i$ . Geometrically, this property implies that the two hyperplanes  $x_i = x_k$  and  $x_j = x_k$  have the same intersection with  $\alpha$ . Similarly, since  $x_i$  and  $x_j$  collide in all of  $\alpha$ , the hyperplane  $x_i = x_j$  plays no role in the cellulation of  $\alpha$ . These two facts allow us to treat  $x_i$  and  $x_j$  as a single particle in  $G$  without changing the hyperplane arrangement. Repeating this process for all particles that share a bracket gives the desired result.  $\square$

**Example 4.4.** Let  $\alpha$  be the intersection of hyperplanes  $x_1 = x_2 = 0$  in  $\mathcal{CB}_5$ . Its diagram looks similar to . The hyperplanes that cellulate  $\alpha$  are all of the hyperplanes of  $\mathcal{CB}_5$ ; however, collisions between  $x_1$  and  $x_2$  are irrelevant to the cellulation (since they are part of the defining hyperplanes of  $\alpha$ ). Furthermore no particle can collide with  $x_1$  or  $x_2$  without also colliding with the fixed particle 0. Thus the remaining hyperplanes, after the redundant ones are removed, are  $x_i = x_j$ ,  $x_i = -x_j$ , and  $x_i = 0$  for all  $i, j > 2$ . Thus  $\alpha$  is cellulated by the  $B_3$  hyperplane arrangement.

4.3. It is easy to check that in most cases the cellulations of hyperplane intersection subspaces  $\alpha$  in Coxeter complexes are indeed other (smaller dimensional) Coxeter complexes. There are, however, three instances where subspaces (intersections of hyperplanes) of the Coxeter complexes  $\mathcal{CD}_n$ ,  $\mathcal{TC}\tilde{B}_n$  and  $\mathcal{TC}\tilde{D}_n$  are not Coxeter complexes themselves. In particular, these subspaces have cellulations combinatorially equivalent to Coxeter complexes with *additional* hyperplanes. We define these three atypical complexes below:

**Definition 4.5.** The complexes of interest are:

1. Let  $\mathcal{CD}_{n,m}$  be  $\mathcal{CD}_n$  with  $m$  additional hyperplanes  $\{x_i = 0 \mid 1 \leq i \leq m\}$ .
2. Let  $\mathcal{TC}\tilde{B}_{n,m}$  be  $\mathcal{TC}\tilde{B}_n$  with  $m$  additional hyperplanes  $\{x_i = 0 \mid 1 \leq i \leq m\}$ .
3. Let  $\mathcal{TC}\tilde{D}_{n,m}$  be  $\mathcal{TC}\tilde{D}_n$  with  $2m$  additional hyperplanes  $\{x_i = 0, 1 \mid 1 \leq i \leq m\}$ .

The configuration space model provides intuition into how these cases arise naturally. Note how these are all complexes with associated configuration spaces on  $\mathbb{R}_o$ ,  $\mathbb{S}_o^\bullet$  and  $\mathbb{S}_o^\circ$ , where not all points along the axis of symmetry have fixed particles. The subspaces of these configuration spaces are those where some particles have collided. In these subspaces, sets of collided particles may be considered in aggregate as a new type of particle, called a *thick* particle. Figure 6(a) shows a bracketing and (b) its representation with thick particles. In general, thick particles allow us to represent any number of coincident particles by a single particle.

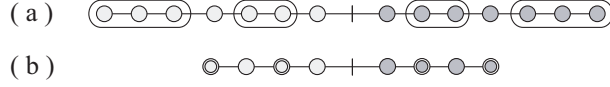


FIGURE 6. Bracketing and thick particles.

Recall that particles were defined such that they could occupy the same point as their inverse; that is, they do not form a collision with their inverse. Unlike (standard) particles, a thick particle and its inverse may not occupy the same point without collision. The reason comes from the hyperplane equations: In the subspace where  $x_i$  and  $x_j$  have collided, the hyperplane  $x_i = -x_j$  represents the same configurations as  $x_i = -x_i (= 0)$ . Note that the number  $m$  of additional hyperplanes added to the complex corresponds to the number  $m$  of thick particles in their configuration spaces. Then the diagram of Figure 6(b) is an element of  $\mathcal{CD}_{4,2}$ , sitting as a subspace of  $\mathcal{CD}_7$  in Figure 6(a).

*Remark.* In the case of non-paired particles, the distinction between standard and thick particles is irrelevant, since no particle has an inverse to collide with. They are also inconsequential in configuration spaces that include a fixed particle at every point where particles may meet their inverses.

4.4. There are natural composition maps on configuration space diagrams that encode the cellulation and stabilizer of a given subspace.

**Definition 4.6.** There are three types of compositions:

- (1) Let  $H$  be a diagram of  $m$  particles of  $C_k(\mathbb{R})$  or  $C_k(\mathbb{S}')$ , with one particle labeled  $i$ . Let  $G$  be a diagram of  $C_k(\mathbb{R})$ . The *composition*  $H \circ_i G$  is the diagram of  $m + k - 1$  particles where the particle  $i$  is replaced by a bracket containing  $G$ .
- (2) Let  $H$  be a diagram of  $m$  paired particles of a configuration space, with one particle labeled  $i$  and its pair labeled  $-i$ . Let  $G$  be a diagram of  $C_k(\mathbb{R})$ . The *composition*  $H \circ_i G$  is the diagram of  $m + k - 1$  paired particles, where the particle  $i$  is replaced by a bracket containing  $G$  and its pair  $-i$  is replaced by a bracket containing the mirror image of  $G$  (left side of Figure 7).
- (3) Let  $H$  be a diagram of a  $m$  paired particles of  $C_{\bar{m}}(\mathbb{R}_{\bullet})$ ,  $C_{\bar{m}}(\mathbb{S}_{\circ}^{\bullet})$  or  $C_{\bar{m}}(\mathbb{S}_{\bullet}^{\bullet})$ , with a fixed particle labeled  $i$ . Let  $G$  be a diagram of either  $C_{\bar{k}}(\mathbb{R}_{\bullet})$  or  $C_{\bar{k}}(\mathbb{R}_{\circ})$ . The *composition*  $H \circ_i G$  is the diagram of  $m + k$  paired particles where the fixed particle  $i$  is replaced by a bracket containing  $G$  (right side of Figure 7).

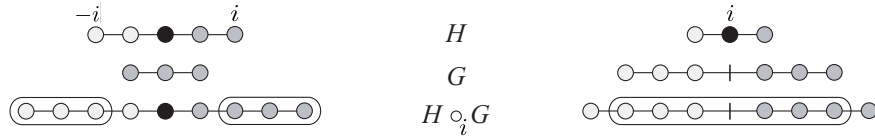


FIGURE 7. Composition operations on bracketings.

Indeed any  $k$ -bracketing  $G$  can be represented as

$$(4.2) \quad G = H \circ_{i_1} G_1 \circ_{i_2} \cdots \circ_{i_k} G_k,$$

where the base  $H$  and the  $G_i$ 's are diagrams without brackets and each  $i_j$  is a particle in  $H$ . From this terminology, the following is a consequence of Lemmas 4.2 and 4.3.

**Proposition 4.7.** *Let  $G$  be a  $k$ -bracketing as defined in Eq.(4.2) and let  $\alpha$  be its support. Then the cellulation of  $\alpha$  is determined by  $H$  and the stabilizer of  $\alpha$  is the product of the configuration spaces diagramed by  $G_1, \dots, G_k$ .*

*Remark.* Table 3 itemizes the collection of 1-bracketings for the spherical cases and Table 4 for the Euclidean ones. In the tables,  $m$  represents the total number of thick particles and  $r$  the number of thick particles in the bracket (stabilizer) of the atypical complexes.

Each valid ordering of particles on the configuration space diagram corresponds to a chamber. We define the *symmetric action*  $\sigma(G)$  on a diagram  $G$  as follows: For a diagram  $G$  with no brackets,  $\sigma$  is the set of all valid permutations of the particles of  $G$ , with those permutations that result in the same chamber identified. Indeed, when  $G$  is a configuration space diagram associated to the spherical or toroidal complex, then  $\sigma(G)$  is simply  $\sigma(W)$ . However if both thick and standard particles are present in the diagram, the group structure breaks down and we are left with just a subset of the symmetric group.

In the case of bracketings, define  $\sigma(G)$  to be the set of permutations of particles which preserve the bracketing; that is, only those reorderings in which the sets of particles sharing a bracket remain unchanged. Thus  $\sigma(G)$  acts independently on each bracket and on the base diagram  $H$  and

$$\sigma(G) = \sigma(H) \times \sigma(G_1) \times \cdots \times \sigma(G_k).$$

This allows us to state a gluing rule for chambers of a closed configuration space.

**Theorem 4.8.** *Let  $G$  be a  $k$ -bracketing as defined in Eq.(4.2). Two faces of different chambers in a closed configuration space, with associated diagrams  $G$  and  $G'$ , are identified if and only if there is an element of  $\sigma(G_1) \times \cdots \times \sigma(G_k)$  taking  $G$  to  $G'$ .*

*Proof.* Geometrically, particles sharing a bracket have already collided. Reordering particles within a bracket has no impact on the configurations represented by  $G$ . Thus all bracketings in the image of  $\sigma(G_1) \times \cdots \times \sigma(G_k)$  correspond to the same cell in the support of  $G$ .

Conversely, two faces of different chambers are identified if they contain the same set of configurations, and thus the same sets of collided particles. Thus  $G$  and  $G'$  have the same diagram, up to reordering of the collided particles. Since  $\sigma(G_i)$  is transitive on each bracket  $G_i$ , the permutation taking  $G$  to  $G'$  is a composition of elements in the  $\sigma(G_i)$ 's.  $\square$

## 5. COMPACTIFICATIONS AND OPERADS

5.1. Compactifying a configuration space  $C_n(V)$  enables the points on  $V$  to collide and a *system* is introduced to record the *directions* points arrive at the collision. In the work of Fulton and

MacPherson [15], this method is brought to rigor in the algebro-geometric context. In [9, Section 4], De Concini and Procesi show that the *minimal blow-ups* of the Coxeter complexes  $\mathcal{CW}$  are equivalent to the Fulton-MacPherson compactifications of their corresponding configuration spaces.

Recall that Kapranov showed the minimal blow-ups of  $\mathcal{CA}_n$  to be isomorphic to the moduli space  $\overline{\mathcal{M}}_{0,n+2}(\mathbb{R})$  [18, Proposition 4.8]. Thus, the Fulton-MacPherson compactification of our configuration spaces yield generalizations of this moduli space. In order to describe these compactified configuration spaces, we begin with definitions.

The collection of hyperplanes  $\{x_i = 0 \mid i = 1, \dots, n\}$  of  $\mathbb{R}^n$  generates the *coordinate arrangement*. A crossing of hyperplanes is *normal* if it is locally isomorphic to a coordinate arrangement. A construction which transforms any crossing into a normal crossing involves the algebro-geometric concept of a blow-up; a standard reference is [17].

**Definition 5.1.** The *blow-up* of a space  $V$  along a codimension  $k$  intersection  $\alpha$  of hyperplanes is the closure of  $\{(x, f(x)) \mid x \in V\}$  in  $V \times \mathbb{P}^{k-1}$ . That is, we replace  $\alpha$  with the projective sphere bundle associated to the normal bundle of  $\alpha$ .

A general collection of blow-ups is usually noncommutative in nature; in other words, the order in which spaces are blown up is important. For a given arrangement, De Concini and Procesi [9, Section 3] establish the existence and uniqueness of a *minimal building set*, a collection of subspaces for which blow-ups commute for a given dimension, and for which every crossing in the resulting space is normal. For a Coxeter complex  $\mathcal{CW}$ , we denote the minimal building set by  $\text{Min}(\mathcal{CW})$ .

**Definition 5.2.** The cellulation  $\mathcal{C}(W)_\#$  is the *minimal blow-up* of  $\mathcal{CW}$ , obtained by blowing up along elements of  $\text{Min}(\mathcal{CW})$  in *increasing* order of dimension.

**Example 5.3.** Figure 8(a) shows the blow-ups of the sphere  $\mathcal{CA}_3$  of Figure 2(a) at nonnormal crossings. Each blown up point has become a hexagon with antipodal identification and the resulting manifold is  $\mathcal{C}(A_3)_\#$ , homeomorphic to the eight-fold connected sum of  $\mathbb{RP}^2$  with itself. Figure 8(b) shows the minimal blow-up of  $\mathcal{CA}_2$  of Figure 3(c).

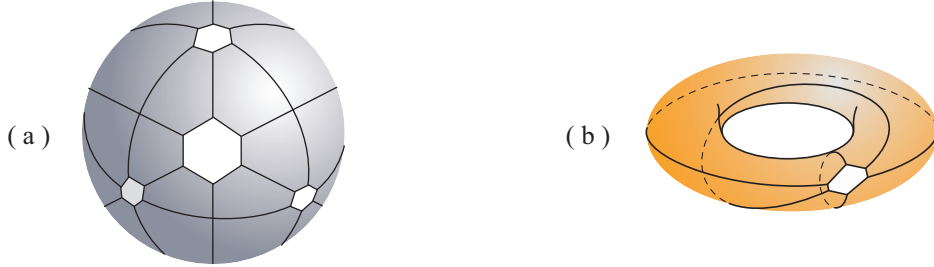


FIGURE 8. Minimal blow-ups of the complexes (a)  $\mathcal{CA}_3$  and (b)  $\mathbb{T}\tilde{A}_2$ .

5.2. The relationship between the set  $\text{Min}(\mathcal{CW})$  and the group  $W$  is given by the concept of reducibility.

**Definition 5.4.** For intersections of hyperplanes  $\alpha, \beta$ , and  $\gamma$ , the collection of hyperplanes  $\mathcal{H}_s \alpha$  is *reducible* if  $\mathcal{H}_s \alpha$  is a disjoint union  $\mathcal{H}_s \beta \sqcup \mathcal{H}_s \gamma$ , where  $\alpha = \beta \cap \gamma$ .

**Lemma 5.5.** [7, Section 3] *Let  $\alpha$  be an intersection of hyperplanes of  $CW$ . Then  $\mathcal{H}_s \alpha$  is irreducible if and only if  $\alpha \in \text{Min}(CW)$ .*

The lemma above can be rewritten in the language of bracketings for the groups  $W$  we are considering here.

**Lemma 5.6.** *Let  $\alpha$  be an intersection of hyperplanes of  $CW$ . Then  $\alpha \in \text{Min}(CW)$  if and only if  $\alpha$  is the support of a 1-bracketing.*

*Proof.* If  $\alpha$  is the support of a 1-bracketing  $G$ , then  $\mathcal{H}_s \alpha$  is determined again by Lemma 4.2. As a result:

1. If  $G$  contains a fixed particle, then  $\mathcal{H}_s \alpha \cong \mathcal{H}B_k$ .
2. If  $G$  contains a particle and its inverse but no fixed particle, then  $\mathcal{H}_s \alpha \cong \mathcal{H}D_k$ .
3. If  $G$  does not contain a particle and its inverse, then  $\mathcal{H}_s \alpha \cong \mathcal{H}A_k$ .

All three of these hyperplane arrangements are irreducible, so  $\alpha \in \text{Min}(CW)$ .

Conversely, let  $\alpha$  be the support of a  $k$ -bracketing  $G = H \circ_{i_1} G_1 \circ_{i_2} \cdots \circ_{i_k} G_k$ . Let  $\beta$  be the support of  $G_1$  and  $\gamma$  be the product of the configuration spaces diagramed by  $G_2, \dots, G_k$ . By the definition of reducibility,  $\mathcal{H}_s \alpha = \mathcal{H}_s \beta \sqcup \mathcal{H}_s \gamma$ , and thus  $\alpha \notin \text{Min}(CW)$  by Lemma 5.5.  $\square$

5.3. As bracketing encoded faces of closed configuration spaces, it is *nested* bracketings which encode faces of compactified configuration spaces [9, Section 2]. Indeed, the codimension  $k$  faces of a chamber of a compactified configuration space are the nested  $k$ -bracketings on the configuration space diagrams. A diagram  $G$  denoted

$$(5.1) \quad G = H \circ_{i_1} G_1 \circ_{i_2} \cdots \circ_{i_k} G_k,$$

is a nested  $(k + m_0 + m_1 + \cdots + m_k)$ -bracketing, where each  $i_j$  is a particle in  $H$  and where  $G_i$  is a nested  $m_i$ -bracketing. The composition maps are those in Definition 4.6. Figure 9 shows an example.

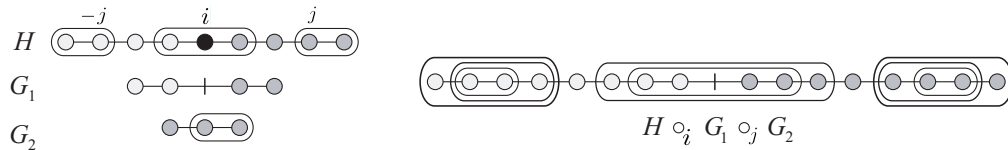


FIGURE 9. Composition operations on nested bracketings.

As before, the support of a nested  $k$ -bracketing  $G$  is the smallest intersection of hyperplanes containing the configurations represented by  $G$ . It is the subspace in which the collisions represented by  $G$  have not only occurred, but have occurred in the order implied by the nesting of brackets in  $G$ . The set of configurations in the support is represented by all reorderings of particles that preserve the bracketing.

**Proposition 5.7.** *Given a nested bracketing  $G$  in a compactified configuration space, the support of  $G$  contains configurations represented by the images of  $G$  under  $\sigma(G)$ .*

*Proof.* From Lemma 5.6, the hyperplanes of  $\mathcal{C}(W)_\#$  correspond to the supports of 1-bracketings. Thus the hyperplanes containing the configurations represented by  $G$  are the hyperplanes corresponding to the brackets in  $G$ . Therefore the support of  $G$  consists of all orderings of particles that respect the brackets of  $G$ . By definition,  $\sigma(G)$  performs these reorderings.  $\square$

5.4. After compactification, different orderings of particles in a bracket do not necessarily represent the same cell. A different action is necessary to describe the identification of diagrams of a projective screen.

**Definition 5.8.** The *flip*  $\hat{\sigma}(G)$  action on an unbracketed diagram  $G$  consists of the identity and the reflection (that reverses the order of the particles of  $G$ ). On a nested bracketing diagram, the action of  $\hat{\sigma}(G)$  acts independently on each component.

**Theorem 5.9.** *Let  $G$  be a nested bracketing corresponding to a compactified configuration space, where*

$$G = H \circ_{i_1} G_1 \circ_{i_2} \cdots \circ_{i_k} G_k.$$

*All bracketings in the image of  $G$  under  $\hat{\sigma}(G_1) \times \cdots \times \hat{\sigma}(G_k)$  represent the same cell.*

*Proof.* By definition, blow-ups introduce a *projective* bundle around each subspace in the minimal building set. The analog in configuration spaces is an identification across each bracket: Flipping the positions of the particles in the bracket is defined to represent the same configuration. Thus the permutations that represent the same set of configurations as  $G$  are exactly the images of  $G$  under  $\hat{\sigma}(G_1) \times \cdots \times \hat{\sigma}(G_k)$ .  $\square$

*Remark.* This theorem gives us a gluing rule between the faces of two chambers. In other words, two nested  $k$ -bracketings  $G_1$  and  $G_2$  of a diagram (representing codimension  $k$ -faces) are identified if  $G_2$  can be obtained from  $G_1$  by flipping some of the brackets of  $G_2$ .

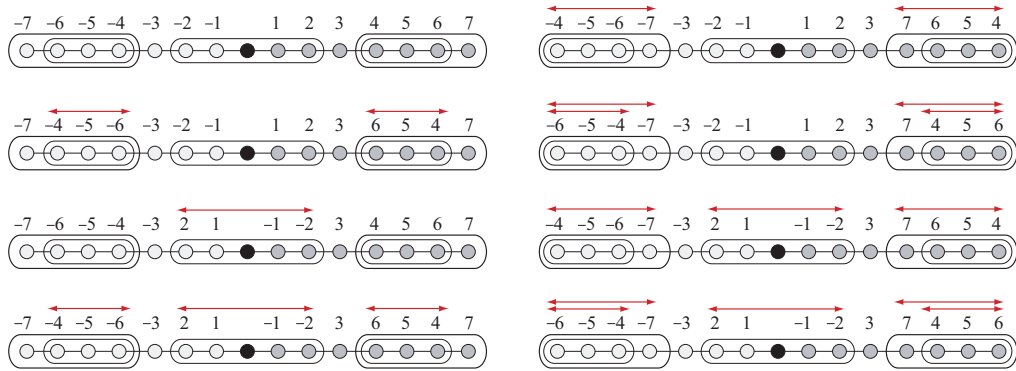


FIGURE 10. Flips on nested bracketings.

Figure 10 shows the permutations that preserve the cell represented by a particular configuration space diagram. Note that reflections commute with each other, and thus they generate a group which is isomorphic to  $(\mathbb{Z}/2\mathbb{Z})^3$ .

5.5. Classically, the notion of an operad was created for the study of iterated loop spaces [27]. Since then, operads have been used as universal objects representing a wide range of algebraic concepts. We give a brief definition; see [20, Section 1] for details.

**Definition 5.10.** An *operad*  $\mathcal{O}$  consists of a collection of objects  $\{\mathcal{O}(n) \mid n \in \mathbb{N}\}$  in a monoidal category endowed with certain extra structures. Notably,

- (1)  $\mathcal{O}(n)$  carries an action by the symmetric group of  $n$  letters.
- (2) There are composition maps

$$\mathcal{O}(n) \otimes \mathcal{O}(k_1) \otimes \cdots \otimes \mathcal{O}(k_n) \rightarrow \mathcal{O}(k_1 + \cdots + k_n)$$

which must be associative, unital, and equivariant.

One can view  $\mathcal{O}(n)$  as objects of  $n$ -ary operations, which yield an output given  $n$  inputs. We will be concerned mostly with operads in the context of topological spaces, where the objects  $\mathcal{O}(n)$  will be equivalence classes of geometric objects. Classically, these objects can be pictured as in Figure 11. The composition  $\mathcal{O}(i) \circ_k \mathcal{O}(j)$  is obtained by grafting the output of  $\mathcal{O}(j)$  to the  $k$ -th input of  $\mathcal{O}(i)$ . The symmetric group acts by permuting the labeling of the inputs.

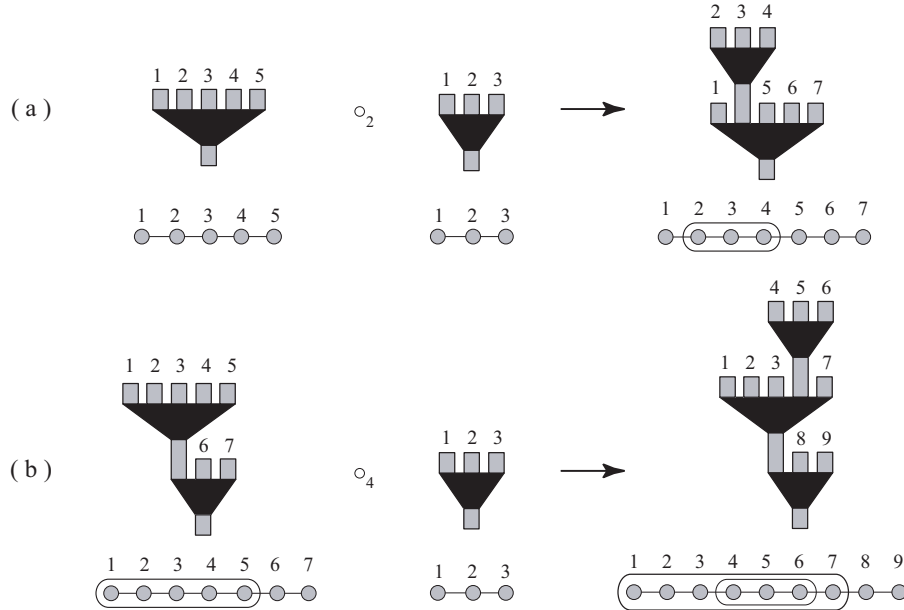


FIGURE 11. Examples of composition maps of an operad, along with dual figures related to (a) bracketing and (b) nested bracketing.

There are several variants to the operad definition above. One classic example is the *non-symmetric* version, which removes all references to the symmetric group in the definition above. Our version, whose naming is credited to J. Stasheff, is as follows:

**Definition 5.11.** Let  $W$  be a Coxeter group from Figure 1. Let  $\mathcal{O}_W(n, k)$  be the collection of configuration spaces of nested  $k$ -bracketings with  $n$  particles associated to  $\mathcal{C}(W)_\#$ .

- (1) The group  $\sigma(W)$  acts on  $\mathcal{O}_W(n, k)$  by permuting the labels.
- (2) There are composition maps

$$\mathcal{O}_W(n_H, k_H) \otimes \mathcal{O}_W(n_1, k_1) \otimes \cdots \otimes \mathcal{O}_W(n_m, k_m) \rightarrow \mathcal{O}_W(n_*, k_*),$$

$$\text{where } n_* = n_H - m + \sum n_i \text{ and } k_* = k_H + m + \sum k_i.$$

This defines the *Coxeter operad*  $\{\mathcal{O}_W(n, k)\}$ .

Note that the composition maps are those described in Eq.(5.1). The group  $\sigma(W)$  is defined in Section 3.3 above.

*Remark.* The Coxeter operad  $\mathcal{O}_A$  leads to the  $A_\infty$  operad structure [27] of the associahedron. The classic symmetric group acting on  $\mathcal{O}_A$  is exactly the  $A_n$  Coxeter group. The affine case  $\mathcal{O}_{\tilde{A}}$  gives the structure of a module over an operad structure [20, Section 4.4]. There is a natural forgetful map from  $\sigma(W)$  to the symmetric group. Thus, the Coxeter operads define classical underlying operads.

Indeed, one can see this operad to be *bi-colored* [21, Section 2]: Intuitively, each of the inputs and output is given one of two colors. An element  $\mathcal{O}(j)$  can be grafted into an input of  $\mathcal{O}(i)$  if and only if the colors of the corresponding input and output match. Our bi-coloring comes from the centrally symmetric axis and free particles. The *tree-like* structure of the Coxeter operad is shown in Figure 12. The affine Coxeter operads are analogous to the spherical ones shown, but an unrooted tree, rather than a rooted one, is used.

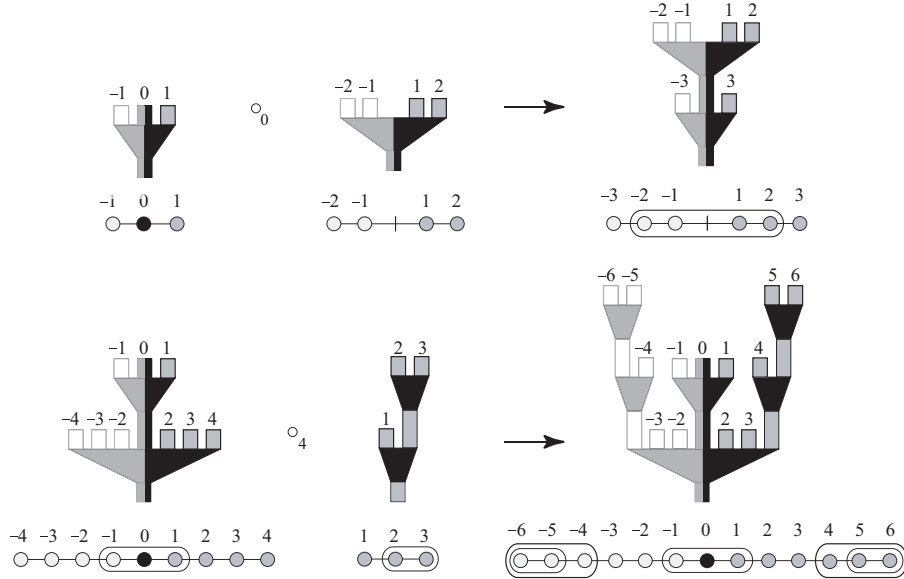


FIGURE 12. Examples of composition maps of the Coxeter operad, along with dual *tree* figures.



*Remark.* There exists a generalization of the classical operad to the *braid* operad, defined by Fiedorowicz, with the braid group playing the role of the symmetric group [13, Section 3]. Since the braid group is the Artin group of type  $A_n$ , it seems plausible that the Coxeter operads above can be extended to their corresponding Artin groups, yielding analogs to the braid operads.

## 6. TILING BY GRAPH-ASSOCIAHEDRA

6.1. This section uses the theory of graph-associahedra developed in [5]. It is applied to the blown-up Coxeter complexes of interest, yielding enumerative results. Notably, the Euler characteristic of these spaces are given.

It is a classic result of geometric group theory that each chamber of a simplicial Coxeter complex is a simplex [4, Section 1]. However, we are interested in the minimal blow-ups of these manifolds.

**Definition 6.1.** Let  $\Gamma$  be a graph. A *tube* is a proper nonempty set of nodes of  $\Gamma$  whose induced graph is a proper, connected subgraph of  $\Gamma$ . There are three ways that two tubes  $t_1$  and  $t_2$  may interact on the graph.

- (1) Tubes are *nested* if  $t_1 \subset t_2$ .
- (2) Tubes *intersect* if  $t_1 \cap t_2 \neq \emptyset$  and  $t_1 \not\subset t_2$  and  $t_2 \not\subset t_1$ .
- (3) Tubes are *adjacent* if  $t_1 \cap t_2 = \emptyset$  and  $t_1 \cup t_2$  is a tube in  $\Gamma$ .

Tubes are *compatible* if they do not intersect and they are not adjacent. A *tubing*  $T$  of  $\Gamma$  is a set of tubes of  $\Gamma$  such that every pair of tubes in  $T$  is compatible. A *k-tubing* is a tubing with  $k$  tubes.

**Theorem 6.2.** [5, Section 3] *For a graph  $\Gamma$  with  $n$  nodes, the graph-associahedron  $\mathcal{P}\Gamma$  is the convex polytope of dimension  $n - 1$  whose face poset is isomorphic to set of valid tubings of  $\Gamma$ , ordered such that  $T \prec T'$  if  $T$  is obtained from  $T'$  by adding tubes.*

Figure 13 shows two examples of graph-associahedra, having underlying graphs as paths and cycles, respectively, with three nodes. These turn out to be the two-dimensional associahedron [27] and cyclohedron [2] polytopes.

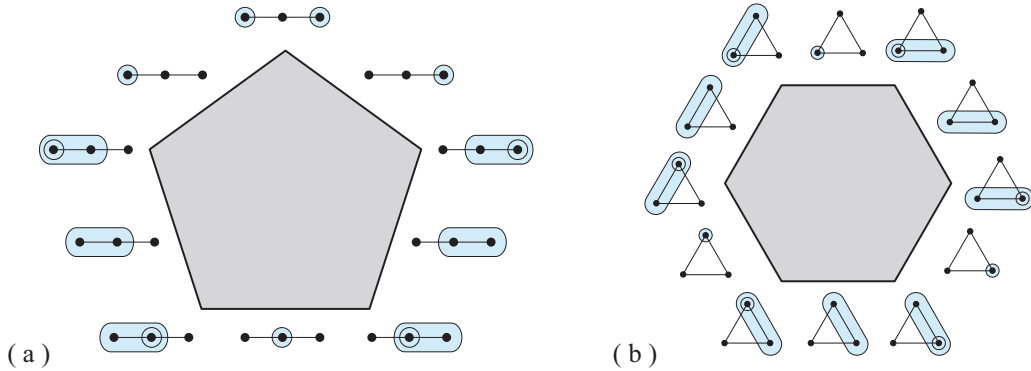


FIGURE 13. Graph-associahedra with a (a) path and (b) cycle as underlying graphs.

**Theorem 6.3.** [5, Section 4] *Let  $W$  be a simplicial Coxeter group and  $\Gamma_W$  be its associated Coxeter graph. Then the  $W$ -action on  $CW_\#$  has a fundamental domain combinatorially isomorphic to  $\mathcal{P}\Gamma_W$ .*

*Notation.* We write  $\mathcal{P}W$  instead of  $\mathcal{P}\Gamma_W$  when context makes it clear.

**Proposition 6.4.** *The tiling of the Coxeter cellulations are given as follows:*

- (1)  $\mathcal{P}A_n$  (the associahedron) tiles  $\mathcal{C}(A_n)_\#$ ,  $\mathcal{C}(B_n)_\#$  and  $\mathbb{TC}(\tilde{C}_{n-1})_\#$ .
- (2)  $\mathcal{P}\tilde{A}_n$  (the cyclohedron) tiles  $\mathbb{TC}(\tilde{A}_n)_\#$ .
- (3)  $\mathcal{P}D_n$  tiles  $\mathcal{C}(D_n)_\#$  and  $\mathbb{TC}(\tilde{B}_{n-1})_\#$ .
- (4)  $\mathcal{P}\tilde{D}_n$  tiles  $\mathbb{TC}(\tilde{D}_n)_\#$ .

*Proof.* For a given graph  $\Gamma$ , the polytope  $\mathcal{P}\Gamma_n$  depends only on the adjacency of nodes, not the label on the edges.  $\square$

*Remark.* There is a natural bijection from the set of all bracketings of a configuration space diagram to the set of all tubings of the associated Coxeter diagram. The bijection is such that two brackets intersect if and only if their images intersect or are adjacent as tubes. Thus the face poset of tubings is isomorphic to the face poset of bracketings, where  $k$  brackets correspond to a codimension  $k$  face. Figure 14 shows some examples of this bijection.

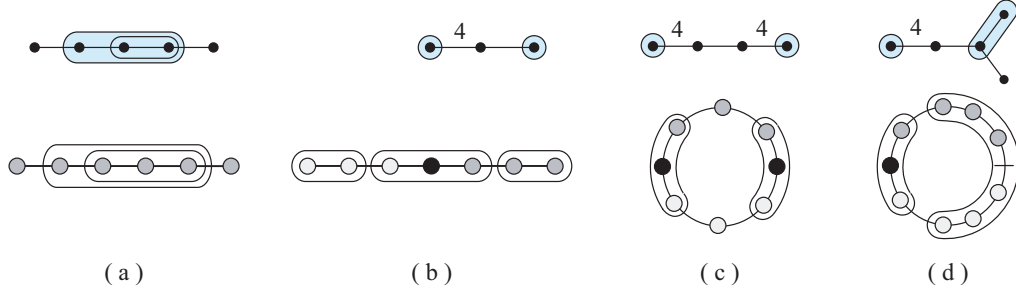


FIGURE 14. Examples of the bijection between tubings and nested bracketings.

6.2. We analyze the structure of these tiling polyhedra  $\mathcal{P}W$ . For a given tube  $t$  and a graph  $\Gamma$ , let  $\Gamma_t$  denote the induced subgraph on the graph  $\Gamma$ . By abuse of notation, we sometimes refer to  $\Gamma_t$  as a tube.

**Definition 6.5.** Given a graph  $\Gamma$  and a tube  $t$ , construct a new graph  $\Gamma_t^*$  called the *reconnected complement*: If  $V$  is the set of nodes of  $\Gamma$ , then  $V - t$  is the set of nodes of  $\Gamma_t^*$ . There is an edge between nodes  $a$  and  $b$  in  $\Gamma_t^*$  if either  $\{a, b\}$  or  $\{a, b\} \cup t$  is connected in  $\Gamma$ .

**Theorem 6.6.** [5, Section 3] *The facets of  $\mathcal{P}\Gamma$  correspond to the set of 1-tubings on  $\Gamma$ . In particular, the facet associated to a 1-tubing  $\{t\}$  is equivalent to  $\mathcal{P}\Gamma_t \times \mathcal{P}\Gamma_t^*$ .*

The facets of  $\mathcal{P}W$  are of the form  $\mathcal{P}\Gamma \times \mathcal{P}\Gamma^*$ , which can be found by simple inspection. Using induction of each term of the product produces the following results:

**Corollary 6.7.** *The faces of  $\mathcal{P}A$  are of the form  $\mathcal{P}A \times \cdots \times \mathcal{P}A$ .*

**Corollary 6.8.** *The faces of  $\mathcal{P}\tilde{A}$  are of the form  $\mathcal{P}\tilde{A} \times \mathcal{P}A \times \cdots \times \mathcal{P}A$ .*

Before moving on to the other tiling polytopes, we need to look at some special graphs which appear as reconnected complements. They are displayed in the Figure 15 below, the subscript  $n$  denoting the number of vertices. Note that the polytope  $\mathcal{P}X_4$  is the 3-dimensional *permutohedron*.

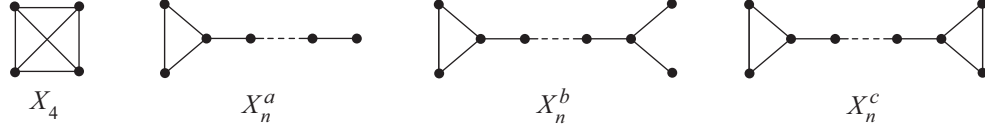


FIGURE 15. Special graphs appearing as reconnected complements.

**Corollary 6.9.** *The faces of  $\mathcal{P}D$  are of the form*

- (1)  $\mathcal{P}A \times \cdots \times \mathcal{P}A$
- (2)  $\mathcal{P}D \times \mathcal{P}A \times \cdots \times \mathcal{P}A$
- (3)  $\mathcal{P}X^a \times \mathcal{P}A \times \cdots \times \mathcal{P}A$ .

**Example 6.10.** Figure 16 illustrates four different polyhedra. The first three are well-known objects: (a) the associahedron  $\mathcal{P}A_4$ , (b) cyclohedron  $\mathcal{P}\tilde{A}_4$  and (c) permutohedron  $\mathcal{P}X_4$ . The last one (d) is  $\mathcal{P}D_4$  with six pentagons  $\mathcal{P}A_3$ , three squares  $\mathcal{P}D_2 \times \mathcal{P}A_2$  and one hexagon  $\mathcal{P}X_3^a$  for facets.

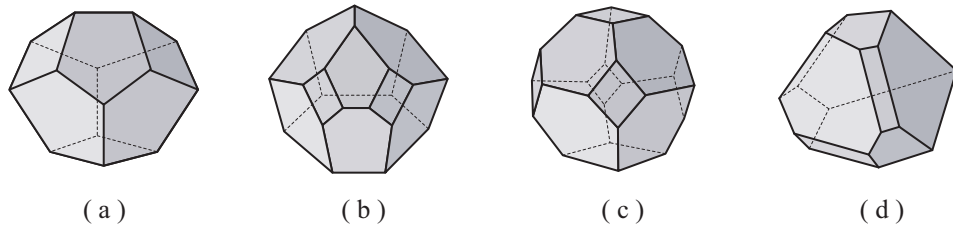


FIGURE 16. The 3-dimensional (a) associahedron  $\mathcal{P}A_4$ , (b) cyclohedron  $\mathcal{P}\tilde{A}_3$ , (c) permutohedron  $\mathcal{P}X_4$  and (d)  $\mathcal{P}D_4$ .

**Corollary 6.11.** *The faces of  $\mathcal{P}\tilde{D}$  are of the form*

- |  |  |
|--|--|
| (1) $\mathcal{P}A \times \cdots \times \mathcal{P}A$   | (6) $\mathcal{P}D \times \mathcal{P}D \times \mathcal{P}A \times \cdots \times \mathcal{P}A$ |
| (2) $\mathcal{P}D \times \mathcal{P}A \times \cdots \times \mathcal{P}A$                         | (7) $\mathcal{P}X^b \times \mathcal{P}A \times \cdots \times \mathcal{P}A$                   |
| (3) $\mathcal{P}X^a \times \mathcal{P}A \times \cdots \times \mathcal{P}A$                       | (8) $\mathcal{P}X^c \times \mathcal{P}A \times \cdots \times \mathcal{P}A$                   |
| (4) $\mathcal{P}X^a \times \mathcal{P}X^a \times \mathcal{P}A \times \cdots \times \mathcal{P}A$ | (9) $\mathcal{P}\tilde{D} \times \mathcal{P}A \times \cdots \times \mathcal{P}A$             |
| (5) $\mathcal{P}D \times \mathcal{P}X^a \times \mathcal{P}A \times \cdots \times \mathcal{P}A$   | (10) $\mathcal{P}X_4 \times \mathcal{P}A \times \cdots \times \mathcal{P}A$ .                |

6.3. We compute the Euler characteristic of the blown-up Coxeter complexes. From Theorem 6.6, we see that the number of codimension  $k$  faces of the polytope  $\mathcal{PW}$  cellulating  $\mathcal{CW}_\#$  is precisely the number of  $k$ -tubings of the associated Coxeter diagram  $\Gamma_W$ .

**Theorem 6.12.** *Let  $f_k(\mathcal{PW})$  be the number of  $k$ -dimensional faces of  $\mathcal{PW}$ , and let  $g$  be the number of chambers in the spherical or toroidal Coxeter complex  $\mathcal{CW}$ . If  $\dim(\mathcal{PW}) = n$ , then*

$$\chi(\mathcal{C}(W)_\#) = \sum_{k=0}^n (-1)^k \frac{g \cdot f_k}{2^{n-k}}.$$

*Proof.* Since all the crossings in  $\mathcal{C}(W)_\#$  are normal, each codimension  $k$  face of  $\mathcal{PW}$  is identified with  $2^k$  copies.  $\square$

*Remark.* The number of vertices in  $\mathcal{PA}$  is the well-known Catalan number [26, Section 6.5]. The faces  $f_k(W)$  of  $\mathcal{PW}$  provide natural generalizations.

Proposition 6.4 shows only four types of graph-associahedra which tile the blown-up Coxeter complexes:  $\mathcal{PA}_n$  (the associahedron),  $\mathcal{P}\tilde{A}_n$  (the cyclohedron),  $\mathcal{PD}_n$  and  $\mathcal{P}\tilde{D}_n$ . The enumeration of the faces of the associahedra  $\mathcal{PA}_n$  is a classic result of A. Cayley [6], obtained by just counting the number of  $n$ -gons with  $k$  non-intersecting diagonals:

$$f_k(\mathcal{PA}_n) = \frac{1}{n+1} \binom{n-1}{k} \binom{2n-k}{n}.$$

The enumeration of face poset of the cyclohedron  $\mathcal{P}\tilde{A}_n$  comes from the work of R. Simion [25, Section 3.1]:

$$f_k(\mathcal{P}\tilde{A}_n) = \binom{n}{k} \binom{2n-k}{n}.$$

In a recent paper, A. Postnikov provides a recursive formula for the generating function of the numbers  $f_k$  [24, Theorem 7.11]. Using this, he has found closed formulas for the graph-associahedra of types  $D_n$  and  $\tilde{D}_n$ . We thank A. Postnikov for sharing the following result:

**Proposition 6.13.** *The face poset enumerations of types  $D_n$  and  $\tilde{D}_n$  are*

$$(6.1) \quad f_k(\mathcal{PD}_n) = 2f_k(\mathcal{PA}_n) - 2f_k(\mathcal{PA}_{n-1}) - f_k(\mathcal{PA}_{n-2}) - f_{k-1}(\mathcal{PA}_{n-1}) - f_{k-1}(\mathcal{PA}_{n-2})$$

and

$$(6.2) \quad \begin{aligned} f_k(\mathcal{P}\tilde{D}_n) &= 4f_k(\mathcal{PA}_{n+1}) - 8f_k(\mathcal{PA}_n) - 4f_{k-1}(\mathcal{PA}_n) + f_{k-2}(\mathcal{PA}_{n-1}) \\ &+ 4f_k(\mathcal{PA}_{n-2}) + 6f_{k-1}(\mathcal{PA}_{n-2}) + 2f_{k-2}(\mathcal{PA}_{n-2}) \\ &+ f_k(\mathcal{PA}_{n-3}) + 2f_{k-1}(\mathcal{PA}_{n-3}) + f_{k-2}(\mathcal{PA}_{n-3}). \end{aligned}$$

**Theorem 6.14.** *The Euler characteristics of the spherical blown-up Coxeter complexes are as follows: When  $n$  is even, the values are zero; when  $n = 2m + 1$  is odd,*

$$(6.3) \quad \chi(\mathcal{C}(A_n)_\#) = (-1)^m 2n ((n-2)!!)^2$$

$$(6.4) \quad \chi(\mathcal{C}(B_n)_\#) = 2^n \frac{1}{(n+1)} \chi(\mathcal{C}(A_n)_\#)$$

$$(6.5) \quad \chi(\mathcal{C}(D_n)_\#) = 2^{n-3} \left[ \frac{8}{n+1} - \frac{1}{n-2} \right] \chi(\mathcal{C}(A_n)_\#).$$

The Euler characteristics of the toroidal blown-up Coxeter complexes are as follows: When  $n$  is odd, the values are zero; when  $n = 2m$  is even,

$$(6.6) \quad \chi(\mathbb{TC}(\tilde{A}_n)_\#) = (-1)^m ((n-1)!!)^2$$

$$(6.7) \quad \chi(\mathbb{TC}(\tilde{B}_n)_\#) = \frac{1}{2(n+1)} \chi(\mathcal{C}(D_{n+1})_\#)$$

$$(6.8) \quad \chi(\mathbb{TC}(\tilde{C}_n)_\#) = 2^n \frac{1}{(n+2)(n+1)} \chi(\mathcal{C}(A_{n+1})_\#)$$

$$(6.9) \quad \chi(\mathbb{TC}(\tilde{D}_n)_\#) = 2^{n-6} \frac{1}{(n+1)} \left[ \frac{64}{n+2} - \frac{15}{n-1} \right] \chi(\mathcal{C}(A_{n+1})_\#).$$

*Proof.* We use Theorem 6.12 to obtain a summation, using the values  $f_k$  given above along with the number of chambers provided by Tables 1 and 2. The values for Eqs.(6.3) and (6.6) have been previously calculated in [10, Section 3.2] and [25, Section 4.3] respectively. Equations (6.4), (6.7) and (6.8) are consequences of Proposition 6.4, where these spaces share the same tiling polytopes as previous calculations.

From Eq. (6.1) and Theorem 6.12, we obtain a linear combination

$$\begin{aligned} \chi(\mathcal{C}(D_n)_\#) &= \frac{2^n}{(n+1)!} \chi(\mathcal{C}(A_n)_\#) - \frac{2^{n-1}}{n!} \chi(\mathcal{C}(A_{n-1})_\#) - \frac{2^{n-3}}{(n-1)!} \chi(\mathcal{C}(A_{n-2})_\#) \\ &\quad + \frac{2^{n-1}}{n!} \chi(\mathcal{C}(A_{n-1})_\#) + \frac{2^{n-2}}{(n-1)!} \chi(\mathcal{C}(A_{n-2})_\#). \end{aligned}$$

Algebraic manipulations result in Eq.(6.5). Similar calculations using Eq. (6.2) yield Eq. (6.9) after simplification.  $\square$

*Remark.* The reason there is a dimension shift between the spherical and toroidal cases is due to the convention of the affine case having  $n+1$  nodes in its Coxeter graph, compared to  $n$  nodes for the spherical.

6.4. The polytopes tiling the minimal blow-ups of the Coxeter complexes are given by Proposition 6.4. We now discuss the tiling of the atypical complexes, given in Definition 4.5, after minimal blow-ups. As in other (compactified) configuration spaces, the chambers of these complexes correspond to orderings of the particles. However, different orderings of particles may give different face posets to the chamber, since switching a standard and thick particle may change the valid bracketings of the diagram. Specifically, near an axis of symmetry with no fixed particles, having thick particles allows more collisions and hence more brackets, than having standard particles. It is here where the polytopes  $\mathcal{P}X^a$ ,  $\mathcal{P}X^b$ , and  $\mathcal{P}X^c$  based on Figure 15 appear.

Recall that the chambers of these complexes arise as subspaces of  $\mathcal{C}(D_n)_\#$ ,  $\mathbb{TC}(\tilde{B}_n)_\#$  or  $\mathbb{TC}(\tilde{D}_n)_\#$ . From Proposition 6.4, these chambers must be *faces* of either  $\mathcal{P}D$  or  $\mathcal{P}\tilde{D}$ . Converting bracketings to tubings allows us to compute the face poset of the chamber using Theorem 6.6. The following is an example of this method. Note how there is not simply one type of polytope tiling each blown-up atypical complex, as was the case with the Coxeter complexes.

**Example 6.15.** By taking different bracketings in configurations  $C_5(\mathbb{R}_o)$  associated to  $\mathcal{C}(D_5)_\#$ , we can produce the configuration space diagrams of different chambers of  $\mathcal{C}(D_{4,1})_\#$ , as in Figure 17.

By converting bracketings to tubings using the bijection, each facet of the chamber corresponds to the appropriate reconnected complement.

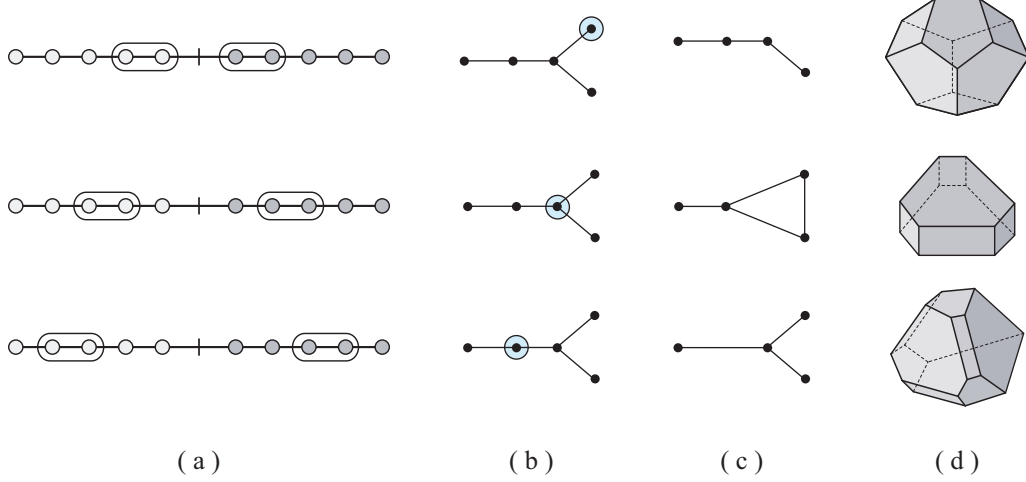


FIGURE 17. (a) Configuration diagram brackets, (b) associated tubing, (c) reconnected complements and (d) fundamental chambers.

The gluing rules for the compactified configuration spaces applies to these atypical models as well. The reflection action can change the ordering of standard and thick particles, and thus it encodes the manner in which polytopes of different types glue to tile the space.

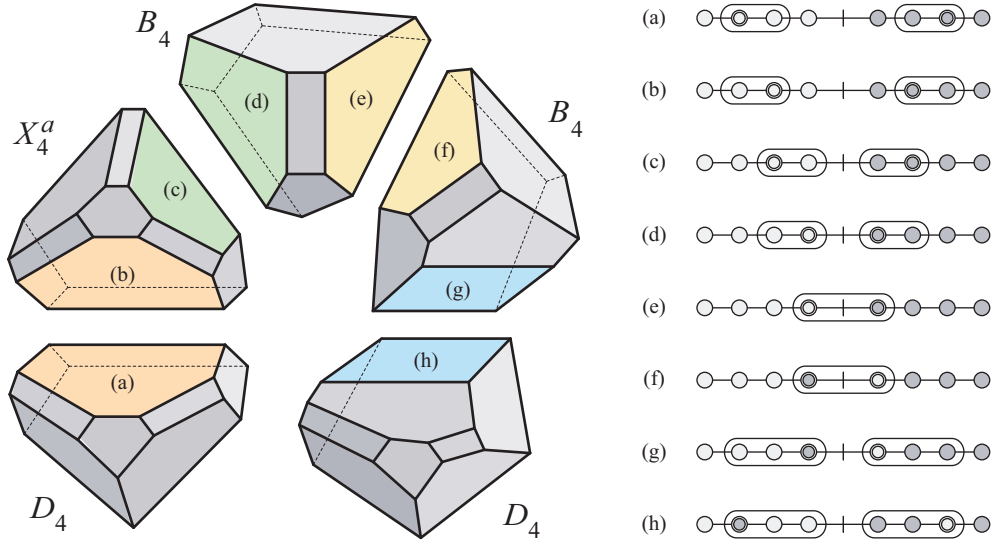


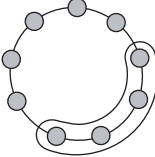
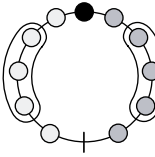
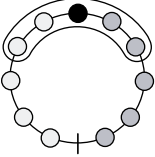
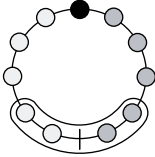
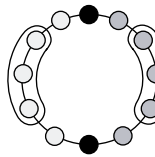
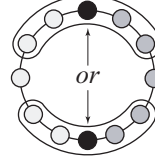
FIGURE 18. Five adjacent chambers in  $\mathcal{C}(D_{4,1})_{\#}$ .

**Example 6.16.** The illustration in Figure 18 of five chambers of  $\mathcal{C}(D_{4,1})_{\#}$  shows how the configuration of three (standard) particles and 1 thick particle encodes gluing of faces among different

types of chambers either across hyperplanes or antipodal maps. This is done by the flip action  $\hat{\sigma}$  of Theorem 5.9. We see the gluing of a face of  $\mathcal{PD}_4$  to a face of  $\mathcal{PX}_4^a$  (a - b) and the corresponding labeled configuration spaces. Another face of this  $\mathcal{PX}_4^a$  attaches to a face of  $\mathcal{PB}_4$  (c - d) which glues to the face of another  $\mathcal{PB}_4$  (e - f). This identification is across the hyperplane  $x_i = 0$ , where  $x_i$  is the label for the thick particle. Finally, this  $\mathcal{PB}_4$  glues to another chamber of type  $\mathcal{PD}_4$  (g - h) through an antipodal map.

| $\mathcal{CW}$       | Cellulation                | Stabilizer    | Enumeration                         | Configuration |
|----------------------|----------------------------|---------------|-------------------------------------|---------------|
| $\mathcal{CA}_n$     | $\mathcal{CA}_{k+1}$       | $A_{n-k-1}$   | $\binom{n+1}{n-k}$                  |               |
| $\mathcal{CB}_n$     | $\mathcal{CB}_{k+1}$       | $B_{n-k-1}$   | $\binom{n}{n-k-1}$                  |               |
|                      | $\mathcal{CB}_{k+1}$       | $A_{n-k-1}$   | $2^{n-k-1} \binom{n}{n-k}$          |               |
| $\mathcal{CD}_n$     | $\mathcal{CB}_{k+1}$       | $D_{n-k-1}$   | $\binom{n}{n-k-1}$                  |               |
|                      | $\mathcal{CD}_{k+1,1}$     | $A_{n-k-1}$   | $2^{n-k-1} \binom{n}{n-k}$          |               |
| $\mathcal{CD}_{n,m}$ | $\mathcal{CB}_{k+1}$       | $D_{n-k-1,r}$ | $\binom{m}{r} \binom{n-m}{n-k-r-1}$ |               |
|                      | $\mathcal{CD}_{k+1,m-r+1}$ | $A_{n-k-1}$   | $2^{n-k-1} \binom{n}{n-k}$          |               |

TABLE 3. Minimal building sets of dimension  $k$  for spherical complexes.

| $CW$          | $\mathbb{TC}\tilde{A}_n$  | $\mathbb{TC}\tilde{B}_n$  |  |   | $\mathbb{TC}\tilde{C}_n$  |   |
|---------------|---|---|--|---|---|---|
| Cellulation   | $\mathbb{TC}\tilde{A}_{k+1}$  | $\mathbb{TC}\tilde{B}_{k+1,1}$  | $\mathbb{TC}\tilde{B}_{k+1}$   | $\mathbb{TC}\tilde{C}_{k+1}$  | $\mathbb{TC}\tilde{C}_{k+1}$  | $\mathbb{TC}\tilde{C}_{k+1}$  |
| Stabilizer    | $A_{n-k}$   | $A_{n-k-1}$   | $B_{n-k}$  | $D_{n-k}$   | $A_{n-k-1}$   | $B_{n-k}$   |
| Enumeration   | $\binom{n+1}{n+1-k}$  | $2^{n-k-1}\binom{n}{n-k}$   | $\binom{n}{n-k}$   | $\binom{n}{n-k}$  | $2^{n-k-1}\binom{n}{n-k}$   | $2\binom{n}{n-k}$   |
| Configuration |  |  |  |  |  |  |

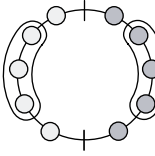
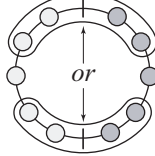
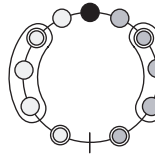
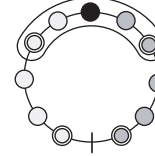
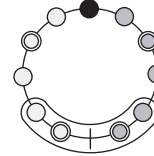
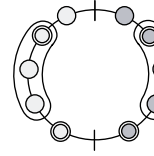
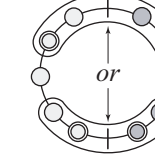
| $CW$          | $\mathbb{TC}\tilde{D}_n$  |   | $\mathbb{TC}\tilde{B}_{n,m}$   |   |   | $\mathbb{TC}\tilde{D}_{n,m}$  |   |
|---------------|---|---|--|---|---|---|---|
| Cellulation   | $\mathbb{TC}\tilde{D}_{k+1,1}$  | $\mathbb{TC}\tilde{B}_{k+1}$  | $\mathbb{TC}\tilde{B}_{k,m-r+1}$   | $\mathbb{TC}\tilde{B}_{k+1,r}$  | $\mathbb{TC}\tilde{C}_{k+1}$  | $\mathbb{TC}\tilde{D}_{k+1,m-r+1}$  | $\mathbb{TC}\tilde{B}_{k+1,r}$  |
| Stabilizer    | $A_{n-k-1}$   | $D_{n-k}$   | $A_{n-k-1}$  | $B_{n-k-1}$   | $D_{n-k-1,r}$   | $A_{n-k-1}$   | $D_{n-k-1,r}$   |
| Enumeration   | $2^{n-k-1}\binom{n}{n-k}$   | $2\binom{n}{n-k}$   | $2^{n-k-1}\binom{n}{n-k}$  | $\binom{n-m}{n-k-r-1}\binom{m}{r}$  | $\binom{n-m}{n-k-r-1}\binom{m}{r}$  | $2^{n-k-1}\binom{n}{n-k}$   | $2\binom{n-m}{n-k-r-1}\binom{m}{r}$   |
| Configuration |  |  |  |  |  |  |  |

TABLE 4. Minimal building sets of dimension  $k$  for Euclidean complexes.



## REFERENCES

1. L. Billera, S. Holmes, K. Vogtmann. Geometry of the space of phylogenetic trees, *Adv. App. Math.* **27** (2001), 733-767.
2. R. Bott and C. Taubes. On the self-linking of knots, *J. Math. Phys.* **35** (1994), 5247-5287.
3. N. Bourbaki. *Lie Groups and Lie Algebras: Chapters 4-6*, Springer-Verlag, Berlin, 2002.
4. K. S. Brown. *Buildings*, Springer-Verlag, New York, 1989.
5. M. Carr and S. Devadoss. Coxeter complexes and graph-associahedra, *Topology Appl.*, to appear.
6. A. Cayley. On the partitions of a polygon, *Proc. Lond. Math. Soc.* **22** (1890), 237-262.
7. M. Davis, T. Januszkiewicz, R. Scott. Nonpositive curvature of blowups, *Selecta Math.* **4** (1998), 491 - 547.
8. M. Davis, T. Januszkiewicz, R. Scott. Fundamental groups of minimal blow-ups, *Adv. Math.* **177** (2003), 115-179.
9. C. De Concini and C. Procesi. Wonderful models of subspace arrangements, *Selecta Math.* **1** (1995), 459-494.
10. S. Devadoss. Tessellations of moduli spaces and the mosaic operad, *Contemp. Math.* **239** (1999), 91-114.
11. S. Devadoss. A space of cyclohedra, *Disc. Comp. Geom.* **29** (2003), 61-75.
12. S. Devadoss. Combinatorial equivalence of real moduli spaces, *Notices Amer. Math. Soc.* **51** (2004), 620-628.
13. Z. Fiedorowicz. The symmetric bar construction, preprint.
14. K. Fukaya, Y-G Oh, H. Ohta, K. Ono. Lagrangian intersection Floer theory: anomaly and obstruction. *Kyoto. Dept. Math.* 00-17.
15. W. Fulton and R. MacPherson. A compactification of configuration spaces, *Ann. Math.* **139** (1994), 183-225.
16. A. Goncharov and Y. Manin. Multiple  $\zeta$ -motives and moduli spaces  $\overline{\mathcal{M}}_{0,n}$ , *Compos. Math.* **140** (2004), 1-14.
17. R. Hartshorne. *Algebraic Geometry*, Springer-Verlag, New York, 1977.
18. M. M. Kapranov. The permutoassociahedron, MacLane's coherence theorem, and asymptotic zones for the  $KZ$  equation, *J. Pure Appl. Alg.* **85** (1993), 119-142.
19. M. Kontsevich and Y. Manin. Gromov-Witten classes, quantum cohomology, and enumerative geometry. *Comm. Math. Phys.* **164** (1994), 525-562.
20. M. Markl, S. Shnider, J. Stasheff. *Operads in Algebra, Topology and Physics*, Amer. Math. Soc., Rhode Island, 2002.
21. M. Markl. Homotopy Algebras are Homotopy Algebras, *Forum Math.* **16** (2004), 129-160.
22. D. Mumford, J. Fogarty, F. Kirwan. *Geometric Invariant Theory*, Springer-Verlag, New York, 1994.
23. T. Parker and J. Wolfson. Pseudo-holomorphic maps and bubble trees. *J. Geom. Anal.* **3** (1993) 63-98.
24. A. Postnikov. Permutohedra, associahedra, and beyond, preprint math.CO/0507163.
25. R. Simion. A type-B associahedron. *Adv. Appl. Math.*, **30** (2003), 2-25.
26. R. P. Stanley. *Enumerative Combinatorics: Volume 2*, Cambridge University Press, New York, 1999.
27. J. D. Stasheff. Homotopy associativity of  $H$ -spaces I, *Trans. Amer. Math. Soc.* **108** (1963), 275-292.

S. ARMSTRONG: WILLIAMS COLLEGE, WILLIAMSTOWN, MA 01267  
*E-mail address:* `suzanne.m.armstrong@williams.edu`

M. CARR: UNIVERSITY OF MICHIGAN, ANN ARBOR, MI 48109  
*E-mail address:* `mpcarr@umich.edu`

S. DEVADOSS: WILLIAMS COLLEGE, WILLIAMSTOWN, MA 01267  
*E-mail address:* `satyan.devadoss@williams.edu`

E. ENGLER: WILLIAMS COLLEGE, WILLIAMSTOWN, MA 01267  
*E-mail address:* `eric.h.engler@williams.edu`

A. LEININGER: MIT, CAMBRIDGE, MA 02139  
*E-mail address:* `anandal@mit.edu`

M. MANAPAT: UNIVERSITY OF CALIFORNIA, BERKELEY, CA 94720  
*E-mail address:* `manapat@ocf.berkeley.edu`